

## Synthesis and Characterization of a New Semiconductor Oligomer Having Quinoline and Fluorene Units

Fábio C. Correia,<sup>a</sup> Thays C. F. Santos,<sup>b</sup> Jarem R. Garcia,<sup>c</sup> Laura O. Peres<sup>b</sup> and Shu H. Wang<sup>\*,a</sup>

<sup>a</sup>*Metallurgical and Materials Engineering Department, Polytechnic School, University of São Paulo (USP), Av. Prof. Luciano Gualberto, 380, 05508-010 São Paulo-SP, Brazil*

<sup>b</sup>*Hybrid Materials Laboratory, Federal University of São Paulo (Unifesp), Campus Diadema, R. Artur Riedel, 275, 09972-270 Diadema-SP, Brazil*

<sup>c</sup>*Chemistry Department, State University of Ponta Grossa (UEPG), Av. Gal. Carlos Cavalcanti, 4748, 84030-900 Ponta Grossa-PR, Brazil*

Um novo material contendo grupos fluoreno e quinolina foi obtido por síntese direta através da reação de Suzuki e mostrou-se ser facilmente solúvel em solventes orgânicos comuns. A estrutura química da macromolécula foi confirmada através da caracterização por medidas de ressonância magnética nuclear de <sup>1</sup>H (<sup>1</sup>H NMR), infravermelho com transformada de Fourier (FTIR), calorimetria diferencial de varredura (DSC), análise termogravimétrica (TGA) e cromatografia de permeação em gel (GPC). Em solução, o material apresentou duas absorções máximas em 314 e 245 nm, juntamente com um alto rendimento quântico de fluorescência (82%) e uma emissão máxima em 419 nm. O band gap do material foi estimado em cerca de 2,60 eV por voltametria cíclica, entretanto o band gap óptico para o filme fino determinado por espectroscopia UV-Vis apresentou valor maior, 3,10 eV. A divergência foi atribuída a interações de transferência de carga, devido à presença de grupos doador e aceptor no copolímero.

A new oligomer having fluorenylene and quinolinylene groups was straightforwardly synthesized by Suzuki reaction and proven to be readily soluble in common organic solvents. The chemical structure of the copolymer was confirmed and characterized by <sup>1</sup>H nuclear magnetic resonance (NMR), Fourier transform infrared (FTIR), differential scanning calorimetry (DSC), thermogravimetric analysis (TGA) and gel permeation chromatography (GPC) measurements. In solution, the oligomer presented two absorption maxima at 314 and 245 nm, along with a high fluorescence quantum yield (82%), characterized by an emission maximum at 419 nm. The band gap of the material was estimated to be around 2.60 eV by cyclic voltammetry, however the optical band gap for the thin film observed by UV-Vis spectroscopy was 3.10 eV. The divergence was attributed to charge transfer interactions due to the presence of donor and acceptor units in the copolymer.

**Keywords:** conjugated material, fluorene, quinoline, Suzuki, OLEDs

### Introduction

Since the discovery of electroluminescence (EL) in conjugated polymers, reported for poly(*p*-phenylene vinylene) (PPV) in 1990,<sup>1</sup> much effort has been done aiming the construction of polymeric light-emitting devices (PLEDs). Polymers allow straightforward processing into large surface area thin films, due to their mechanical flexibility and toughness, low-cost manufacturing through solution-processing, among other benefits.<sup>2,3</sup>

It is well known that the performance of PLEDs is still limited by the number of electron/hole recombinations that is influenced by the number and the mobility of the charge carriers in the given constitutive layer of the device and, additionally, dictates the optimum applied voltage and the lifetime of the devices.<sup>4</sup> Most of the EL semiconducting polymers have properties of injecting and transporting holes more efficiently than electrons.<sup>5</sup> Thus, synthesis of novel efficient electron transport polymers presenting good emitting properties might improve device performance, by eliminating an electron injection layer, incrementing the number of charge carrier recombination and reducing the threshold voltage.

\*e-mail: wangshui@usp.br

Quinoline and its derivatives, specially tris(8-hydroxyquinoline)aluminum (Alq3), are known for their good properties as electron injecting and transporting layer, which are attributed to its n-type conducting nature. The optical and electronic properties of quinoline derivatives have been studied extensively,<sup>6</sup> including optical studies of quinoline-containing polymer connected with protonation and metal cation coordination.<sup>7</sup> Those polymers have shown excellent mechanical properties, high thermal stability and processability into high-quality thin films and, recently, some quinolines were demonstrated to be suitable for the fabrication of light-emitting diodes (LEDs).<sup>8</sup> However, the reported quinoline polymers were prepared by complex synthesis procedures and are characterized by low solubility in ordinary organic solvents.<sup>9-14</sup>

Polyfluorenes and their derivatives, on the other hand, are the prevailing blue light-emitting materials for PLEDs, due to their high photoluminescence (PL) and EL, excellent thermal and oxidative stability and good solubility in common organic solvents. Additionally, the 9-position of fluorene offers the ability to control interactions among chains through functionalization, leading to tailored electrical and optical properties, which are exemplified by numerous fluorene copolymers with excellent thermal stability, reduced turn-on voltage and enhanced EL.<sup>15-18</sup>

Therefore, fluorene-based copolymers containing quinoline units emerge as promising materials in organic LEDs. Such sort of copolymers has been prepared with acid-catalyzed Friedländer quinoline synthesis through condensation reactions of bis(*o*-aminoketone)s and bisacetyl groups,<sup>19-21</sup> and proved to present interesting optical properties and good thermal stability. The copolymers have been applied in multilayer LEDs as the emissive layer as well as the electron transport layer (ETL), and improvement of the LED performance has been reported.<sup>19,20</sup>

In the present work, a new material was easily synthesized by the copolymerization of dihalogenated quinoline and fluorene monomers with 1,4-phenylenebisboronic acid, using a palladium-catalyzed Suzuki coupling reaction.<sup>22</sup> This is a typical reaction between organoboron compounds with different types of organic electrophile and organic halides. One additional advantage of these reactions includes mildness of the reaction conditions, great tolerance

toward a variety of functional groups and insensitiveness to the presence of water.<sup>23,24</sup>

## Experimental

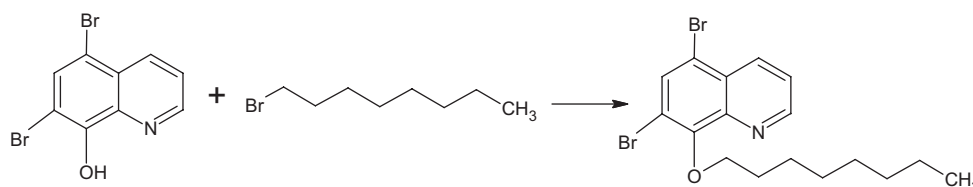
All reagents were used as received from commercial sources (Aldrich or Acros) and used without further purification.

### Synthesis of 5,7-dibromo-8-oxyoctyl-quinoline

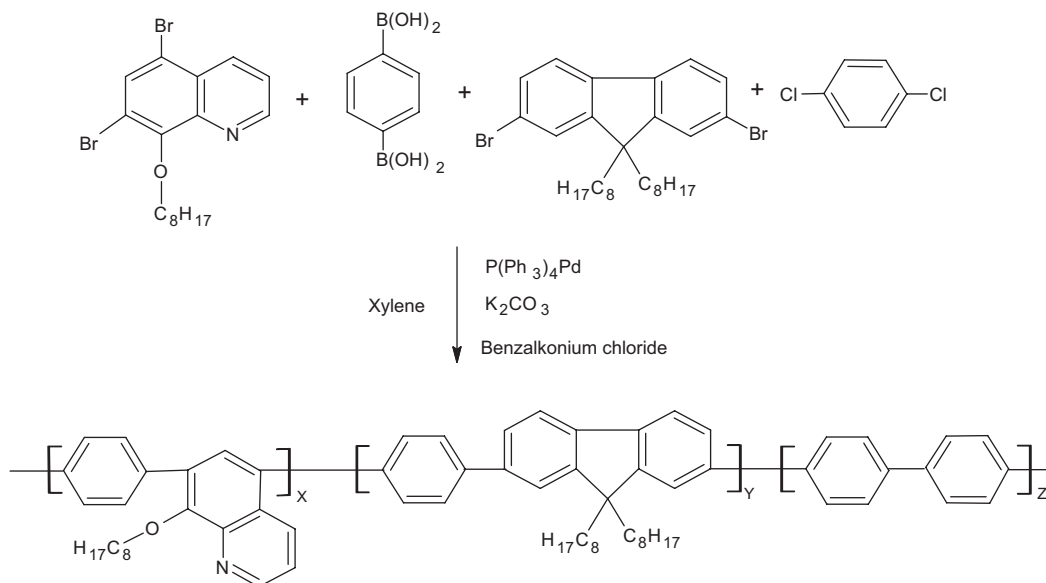
In a one-neck flask, a solution containing 150 mL of dimethylformamide, 5,7-dibromo-8-hydroxyquinoline (15.1 g, 0.05 mol) and 1-bromooctane (11.5 g, 0.06 mol), anhydrous potassium carbonate ( $K_2CO_3$ ) (15 g, 0.11 mol) was added portion-wise to the mixture for 1 hour (Scheme 1). The solution was allowed to react under nitrogen atmosphere and magnetic stirring at 100 °C for 12 h.<sup>25</sup> After this period, the mixture was cooled to room temperature and poured into a mixture of ethanol and distilled water (10:1). The product (off-white needles) was recrystallized from an ethanol:water mixture, filtered and dried in a vacuum oven. Yield 18.5 g (90%); <sup>1</sup>H nuclear magnetic resonance (NMR) (200 MHz,  $CDCl_3$ )  $\delta$  8.98 (1H, N-CH), 8.44 (1H, Br-CH), 8.01-7.26 (2H, Ar-H), 4.36 (2H, O-CH<sub>2</sub>), 1.94-1.29 (12H, H-CH<sub>2</sub>), 0.88 (3H, CH<sub>3</sub>).

### Synthesis of poly[1,4-phenylene-2,7-(9,9-dioctyl-fluorenylene)-co-1,4-phenylene-5,7-(8-oxyoctyl-quinolinylene)] (PFQ)

The oligomer was prepared (Scheme 2) following procedures described in the literature.<sup>25</sup> In a three-neck flask, 5,7-dibromo-8-oxyoctyl-quinoline (0.586 g, 1.419 mmol), 1,4-phenylenebisboronic acid (0.334 g, 2.015 mmol), 9,9-dioctyl-2,7-dibromofluorene (0.108 g, 0.197 mmol), 1,4 dichlorobenzene (0.058 g, 0.394 mmol) and  $Pd(PPh_3)_4$  (0.034 mg, 3 mol%) were added to a degassed mixture of xylene (15 mL), benzalkonium chloride (0.1791 g) and 10 mL of 2 mol L<sup>-1</sup>  $K_2CO_3$ . The mixture was vigorously stirred at 100 °C for 48 h under nitrogen atmosphere. Then, phenylboronic acid (0.0626 g, 0.5 mmol) was added as an end-capping agent to the mixture and heated for an additional 12 h. After cooling to room temperature, the



**Scheme 1.** Synthesis of 5,7-dibromo-8-oxyoctyl-quinoline.



**Scheme 2.** Synthesis of PFQ, where  $x = 0.7$ ,  $y = 0.1$  and  $z = 0.2$  are the molar fractions.

oligomer was dissolved in chloroform and precipitated in methanol three times. The yellowish precipitate was filtered and dried in a vacuum oven. Yield 0.552 g (88%).  $^1H$  NMR (200 MHz,  $CDCl_3$ )  $\delta$  8.92-8.97 (1H, N-CH), 8.5-7.2 (24H, Ar-H), 4.10-4.00 (2H, O-CH<sub>2</sub>), 2.05-1.95 (12H, CH<sub>2</sub>), 1.70-1.08 (34H, CH<sub>2</sub>), 0.89-0.77 (9H, CH<sub>3</sub>).

### Characterization

The molar mass and the polydispersity of PFQ were determined by gel permeation chromatography (GPC) using a Waters high performance liquid chromatography (HPLC) system, comprised by two columns in series, PLgel mixed-B and PLgel mixed-C, at 35 °C and flow rate of 1 mL min<sup>-1</sup> of tetrahydrofuran (THF). The GPC measurements are reported using monodisperse polystyrene samples as standards.

The  $^1H$  NMR spectra (200 MHz) of the monomers and PFQ were recorded using a Bruker AC-200 spectrometer with deuterated chloroform (Aldrich) as solvent and tetramethylsilane (TMS) as internal reference.

The Fourier transform infrared (FTIR) spectra of the monomers and copolymer were recorded as solid thin films deposited on a KBr window, using a Bruker FTIR spectrometer, model Vector 22.

The thermal properties of PFQ were investigated by thermogravimetric analysis (TGA) and differential scanning calorimetry (DSC). TGA curves were obtained by using a thermogravimetric analyzer TGA-51 (Shimadzu), in the range from 50 to 800 °C at a heating rate of 10 °C min<sup>-1</sup> under argon atmosphere, and DSC curves were obtained by using a TA Instruments differential scanning calorimeter,

model Q100, in the range from -80 to 180 °C at a heating rate of 10 °C min<sup>-1</sup> under nitrogen atmosphere.

UV absorption spectra were collected using a Cary 50 Conc (Varian) spectrophotometer. Each sample was dissolved in chloroform and the solution was poured into a 10 mm<sup>2</sup> quartz cell. The transmission spectrum was collected from 200-600 nm. PL spectra in solution were determined using a Varian Eclipse fluorescence spectrophotometer. Each sample was dissolved in chloroform and subjected to irradiation at the absorption maximum observed by UV spectroscopy and the emission spectra were collected accordingly.

Microanalysis was performed using a Philips scanning electron microscope, model XL-30, equipped with an energy dispersive X-ray analyzer (EDX) in order to check the atomic composition of PFQ and the presence of halogen as impurity.

Cyclic voltammetric (CV) measurements were carried out using a conventional one-compartment electrochemical cell, with platinum (Pt) wire as the working electrode; a graphite sheet was used as the counter electrode and Ag/Ag<sup>+</sup> as a quasi-reference electrode. The electrolyte was composed of a solution of 0.1 mol L<sup>-1</sup> tetrabutylammonium perchlorate (TBAP) in acetonitrile, containing 5.0 mg L<sup>-1</sup> of the oligomer. N<sub>2</sub> was bubbled through the system, shortly before measurements, in order to remove any dissolved O<sub>2</sub>.

## Results and Discussion

The new material PFQ was synthesized successfully according to Scheme 2, with good yield (88%). PFQ was

obtained as a faint yellow color solid, readily soluble in common organic solvents, such as  $\text{CHCl}_3$ ,  $\text{CH}_2\text{Cl}_2$  and THF. The good solubility of PFQ is attributed to the 8-oxyoctyl group attached to the quinolone unit. The molar mass value ( $M_w$ ), 2780  $\text{g mol}^{-1}$ , determined by GPC, with a polydispersity of 1.89, indicates that just oligomeric structure was obtained. This result can be explained by the presence of bulky groups, substituted quinoline and fluorene units, leading to steric hindrance and difficulty in the C–C bond formation. The low molecular weight aids the solubility issue. However, many conjugated polymers like poly(*p*-phenylene vinylene) (PPV), poly(*p*-phenylene) (PPP) and polyfluorene (PF) are insoluble due to the bulky groups, even with relatively low  $M_w$ . Some strategies are used to make these materials soluble. One of them is to insert an aliphatic group in the fully aromatic backbone. In the case of PFQ, we believe that the modification of quinoline and fluorene with aliphatic groups benefits this property.<sup>26</sup> In the literature, there are some substituted polyfluorenes that are also soluble in organic solvents.<sup>27</sup>

The infrared spectrum of PFQ is shown in Figure 1 in two different regions. The region between 1900 and 2700  $\text{cm}^{-1}$  is not shown here, as no significant band could be pointed out. In the first region, with high wavenumber values, the high intensity bands at 2960 and 2926  $\text{cm}^{-1}$  are assigned to C–H stretching vibrations from  $\text{CH}_3$  aliphatic groups, while the band at 2854  $\text{cm}^{-1}$  is assigned to C–H of methylene groups. Polynuclear aromatic hydrocarbons, on the other hand, display weak C–H stretching bands in this region, however at higher frequencies, here observed at 3025 and 3060  $\text{cm}^{-1}$ . In the second region, between 600 and 2000  $\text{cm}^{-1}$ , no characteristic bands of the starting materials, such as the boronic group, are recognized. The absorptions due to the B–O bond should appear between 1330 and 1350  $\text{cm}^{-1}$  if the copolymerization, using the palladium-catalyzed Suzuki coupling reaction, was incomplete. The absence of this band, as highlighted in Figure 1b, demonstrates that the whole synthetic process successfully removed the boronic groups from the polymer chain terminations. These groups, if present, could act as electron traps, reducing the efficiency of the light-emitting devices.<sup>28</sup> The absorption band around 1600  $\text{cm}^{-1}$  is characteristic, originating from the stretching vibration mode of the C=N bonds, indicating that the quinoline units were incorporated in PFQ by the polymerization process.

EDX analysis (Figure 2) was performed in order to check the presence of surplus chemical elements in the structure of PFQ. Through this spectrum, it was possible to prove the absence of chlorine and boron, and low level of bromine, indicating that the purification process successfully eliminated these impurities from the final

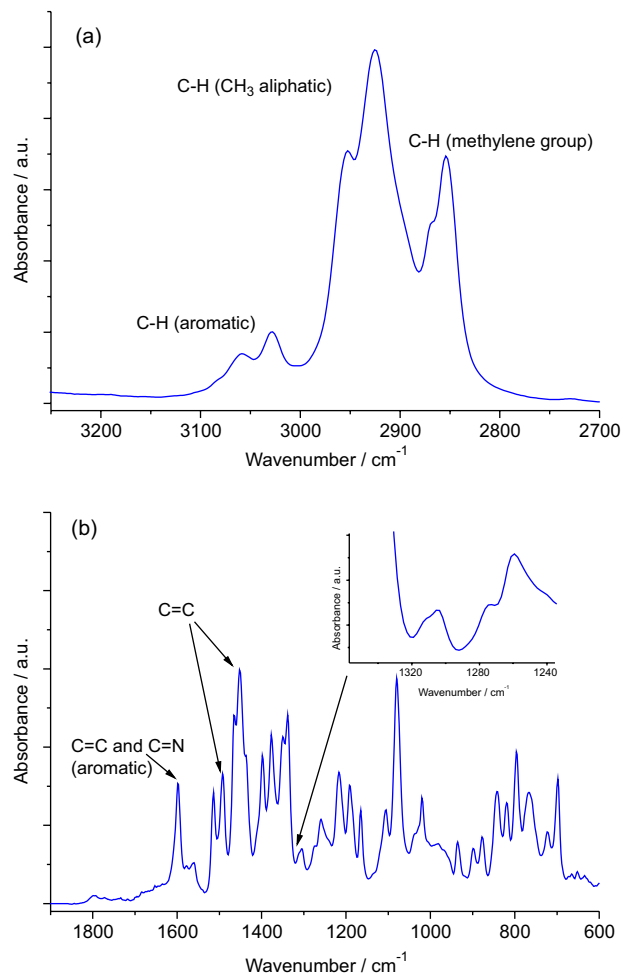


**Figure 1.** FTIR spectrum of PFQ in two regions, (a) 2700 to 3300  $\text{cm}^{-1}$  and (b) 1900 to 600  $\text{cm}^{-1}$ .

product and also confirming the data showed by infrared spectroscopy.

Figure 3 shows the TG and DTG curves for PFQ. TGA reveals good polymer thermal stability with the decomposition temperature onset at 336  $^{\circ}\text{C}$  under a nitrogen atmosphere. The DSC curve shows a glass transition temperature ( $T_g$ ) at 28  $^{\circ}\text{C}$  for PFQ. This  $T_g$  value is close to that observed for typical polyfluorenes (55  $^{\circ}\text{C}$ ),<sup>29,30</sup> however its lower value can be explained as a result of the attachment of two octyl groups onto the C-9 position of the fluorene unit.

The photophysical behavior of PFQ, UV-Vis absorption and emission, were investigated in  $\text{CHCl}_3$  solution and as a thin solid film. Figures 4 and 5 show the UV-Vis and PL spectra, respectively, in comparison with those of the starting compounds, 5,7-dibromo-8-oxyoctyl-quinoline and 9,9-dioctyl-2,7-dibromofluorene.

The UV-Vis spectrum of PFQ is a result of absorptions due mainly to the fluorenylene-phenylene, polyphenylene and quinolinylene-phenylene segments in the oligomer

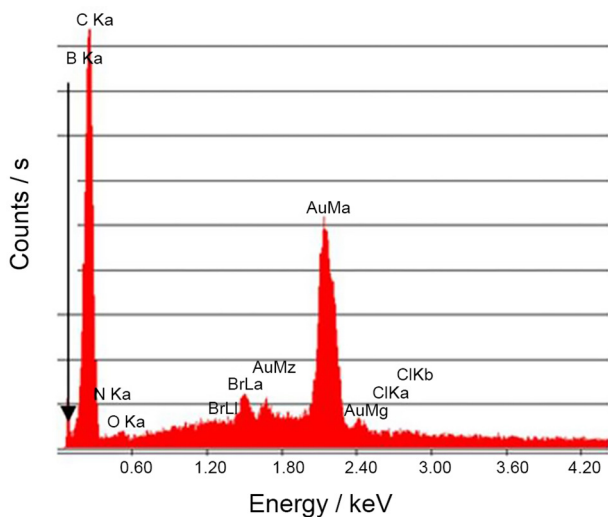


Figure 2. EDX of PFQ.

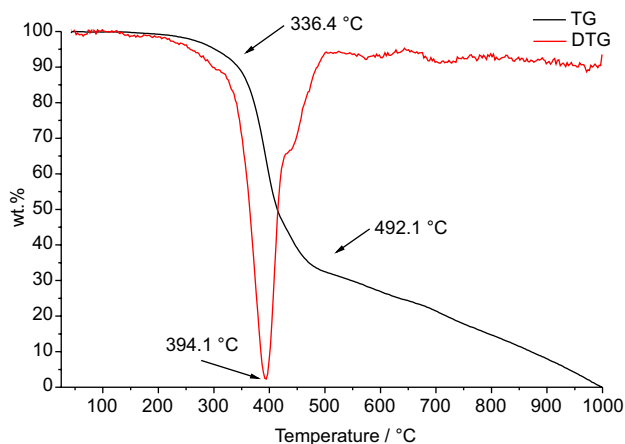


Figure 3. TGA and DTG curves for PFQ.

backbone, which have changed in comparison with those of dibromofluorene and dibromoquinoline, respectively, indicating that polymerization was accomplished (Figure 4).

It is well known that benzene displays 3 absorption bands, namely, 184 nm ( $\epsilon_{\max}$  60,000), 204 nm ( $\epsilon_{\max}$  7,900) and 256 nm ( $\epsilon_{\max}$  200), originated from  $\pi \rightarrow \pi^*$  transitions. The first band is an allowed transition, while both weaker bands are due to forbidden transitions. The absorption at the longest wavelength is characterized to present vibrational fine structure dependent on the physical state and solvent polarity. Substitution on the benzene ring is known to provoke bathochromic shift, specially the attachment of unsaturated and aromatic groups, therefore the phenylene absorptions in PFQ are expected to be swamped by the more intense bands due to quinolinylene and fluorenylene groups.

The fluorene solution absorption spectrum<sup>31</sup> also shows three distinct groups of bands, a moderately intense band near 300 nm, followed by a stronger more complex region

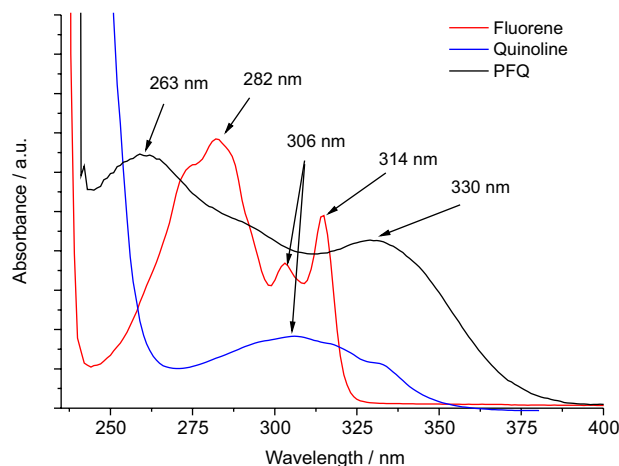


Figure 4. UV-Vis spectrum of PFQ, 5,7-dibromo-8-oxyoctyl-quinoline (quinoline) and 9,9-dioctyl-2,7-dibromofluorene (fluorene) in chloroform.

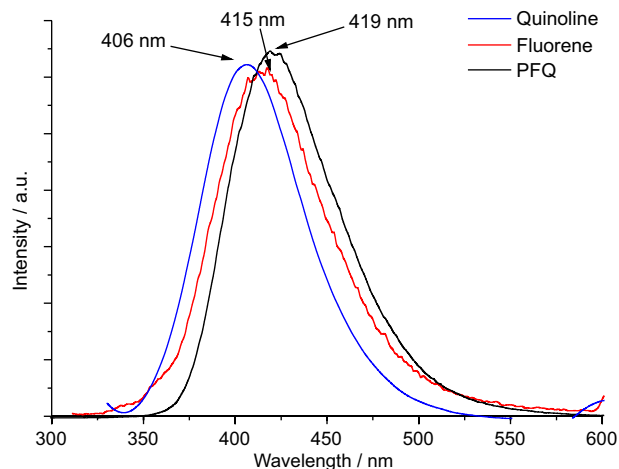


Figure 5. PL spectrum of PFQ, dibromo-8-oxyoctyl-quinoline (quinoline) and 9,9-dioctyl-2,7-dibromofluorene (fluorene).

of absorption at about 260 nm and an even stronger system beginning near 230 nm. The absorptions are attributed to  $\pi \rightarrow \pi^*$  transitions originated from A1 (short-axis polarized) and B2 (long-axis polarized) states. Regarding the substitution effects of auxochromic groups in the 2 and 7 positions (near the long axis) of fluorene, also bathochromic shifts were previously reported.<sup>32</sup> For 9,9-dioctyl-2,7-dibromofluorene (Figure 4), the two regions at longer wavelength presented complex structures and maxima,  $\lambda_{\max} = 282$  and 314 nm, respectively, and are observed to be red-shifted from those of fluorene due to the presence of the bromo and the *n*-octyl substituents, as expected.

Quinoline is a heteroaromatic compound, so the  $n \rightarrow \pi^*$  and the  $\pi \rightarrow \pi^*$  transitions are expected to be shown, however the band due to the  $n \rightarrow \pi^*$  transition is generally weak, while the bands associated with the  $\pi \rightarrow \pi^*$  transitions do not present fine structure and are observed in two regions, which cover up the band owed to the  $n \rightarrow \pi^*$  transition and showed two maximum absorption

peaks at 330 and 263 nm. In comparison with the starting materials, it is possible to verify that the maximum peak at 330 nm for the PFQ is red-shifted, as 314 nm for fluorene and 306 nm for quinoline are the maxima in the longer wavelength region, furthermore, PFQ exhibits a band-broadened absorption even if the profile is similar to the quinoline band at 306 nm.

From an analysis of the absorption spectra and using the relationship  $E = hc / \lambda$ , it is possible to evaluate the optical band gap energy. The wavelength used is that obtained from the onset of the UV-Vis absorption band for PFQ and the value found was 3.10 eV.

In Figure 5, it is possible to observe the characteristic emission peak for each material in solution. For quinoline, the maximum emission peak was at 406 nm and for fluorene, at 415 nm, values very close to that found for PFQ, at 419 nm. Both starting materials presented a broad emission band in the visible range of the electromagnetic spectrum. The PL spectrum of PFQ was dominated by emissions from the fluorene excimer and the PL quantum yield (88%) was determined using quinine sulfate standard. For all materials, different excitation wavelengths were applied, namely 330, 314, 282 and 263 nm, with maximum intensity peak observed after excitation at 314 nm (first maximum absorbance peak). The fluorescence intensity was observed to vary although the wavelength of the emission peak remained constant for each substance, demonstrating an individual emission center for each one.

The PL in solid state (Figure 6) was investigated on thin films prepared by spin-coating from chloroform solution. Differently from the solution, the thin film emission spectra showed well-resolved structural features with maxima at 407, 430 and 465 nm, assigned to the 0-0, 0-1, and 0-2 singlet transitions, respectively (the 0-0 transition being the most intense).<sup>33</sup> Moreover, the maximum of the more intense

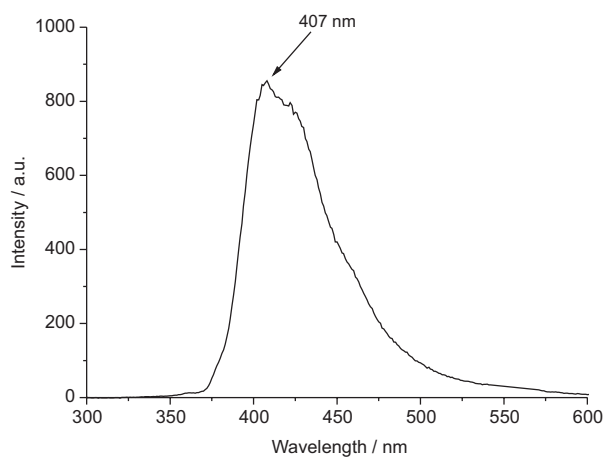


Figure 6. PL spectrum of PFQ in thin film.

emission peak at 407 nm is 12 nm blue-shifted in comparison with the maximum observed for the oligomer in solution. This behavior could be assigned to the diminishment of the effective conjugation length during the solid state formation due to the low molar mass of the oligomers studied (approximately 3 distinctive units, see Scheme 2). Furthermore, the resolved structural feature observed in the solid state emission is caused by the increase on the stiffness of the oligomer structure in the solid state.

The electrochemical behavior of the oligomer dissolved in an electrolyte solution (0.1 mol L<sup>-1</sup> TBAP in acetonitrile) was investigated by CV (Figure 7) and the oxidation and reduction potentials derived from the onset of redox curves in the cyclic voltammograms were determined and the results are summarized in Table 1. In Figure 7, two irreversible reduction peaks, potentials ( $E_{p,c}$ ) at -0.55 and -1.25 V, are shown in the first polarization cycle, associated to the n-doping process. The first reduction peak is related to the presence of the quinoline units and indicates a higher electron affinity for this copolymer unit in comparison with fluorene homopolymers. As the oligomer structure presents different constitutive units, it is coherent to assume that these units may give rise to distinctive responses under electrochemical n- and p-doping processes. Following this reasoning, the second reduction peak could be assigned to the fluorene-alt-phenylene moieties. In the second cycle, the first reduction peak is shifted to a more negative potential resulting in a  $E_{p,c} = -0.8$  V, however the second one maintained its  $E_{p,c}$  at -1.25 V, although all current quantities were observed to reduce. This decrease in the current observed in the second cycle compared to the first one is frequently observed and is due to the hysteresis behavior of the mass transference progression on the electrode surface and to the conformational changes in the polymer/oligomer chains. A similar behavior is observed in the positive

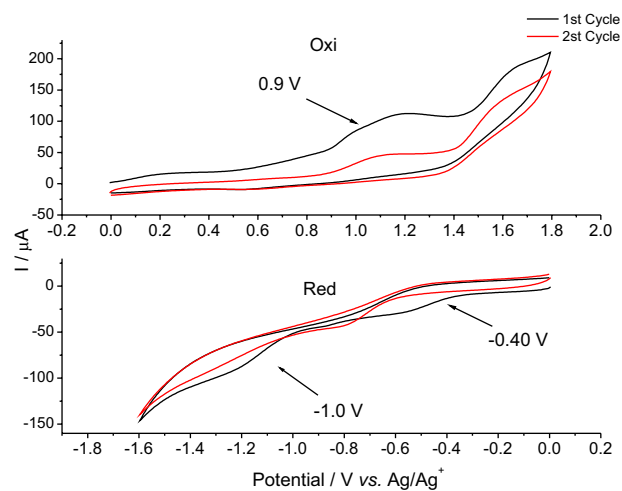


Figure 7. Cyclic voltammogram of PFQ.

potential range of the voltammetric measurements. In the first cycle, two irreversible oxidation peaks are present, one at  $E_{p_c} = 1.20$  V (in fact, the first peak also presents a shoulder at  $E_{p_c} = 1.0$  V) and the other at  $E_{p_c} = 1.65$  V. There is no shift for the  $E_{p_c}$  values during the second cycle, but the current intensities decreased, as already observed in the negative potential range. The first oxidation peak is related to the presence of the quinoline units and the second one is assigned to the fluorene-alt-phenylene segments.

The band gap energy of this material could be determined by the onset of the redox bands in the cyclic voltammetry experiments. The ionization potential (IP) and electron affinity (EA) energies of the oligomeric structure are calculated according to the empirical formula:  $IP = -(E_{\text{onset-ox}} + 4.7)$  eV and  $EA = -(E_{\text{onset-red}} + 4.7)$  eV, taking into account one electron transfer and the conditions of this experiment (Ag/Ag<sup>+</sup> reference electrode, 0.1 mol L<sup>-1</sup> TBAP in acetonitrile).<sup>34</sup> As previously described, under cyclic voltammetry, the oligomer in solution presented two processes in the reduction curves and the same in the oxidation curves. The processes occurring under the lower applied voltage, independently of being a reduction or an oxidation event, were assigned to the presence of the quinoline units. In this case, the reduction and oxidation processes involve the O and N atomic orbitals<sup>35</sup> as  $n \rightarrow \pi^*$  transitions are induced, although such electronic transitions do not imply in noteworthy optical properties in the oligomers. In fact, that the  $n \rightarrow \pi^*$  transition is "forbidden" by symmetry considerations (low molar absorptivities ( $\epsilon$ ),  $\leq 100$ ), thus the intensity of the band due to this transition is low. Moreover, in conjugated systems, this transition undergoes a red shift with little change in intensity, which in the absorption spectrum is overlapped by the long-wavelength shoulder of the  $\pi \rightarrow \pi^*$  transition.<sup>36</sup> For the reasons exposed above, the band gap energy was calculated using the  $E_{\text{onset}}$  values for the redox process occurring in the higher potential region in the CV experiments.

Thus, considering that the values of the  $E_{\text{onset-ox}} = 1.55$  V (the value reported for polyfluorene homopolymer is around 1.35 V)<sup>33</sup> and  $E_{\text{onset-red}} = -1.05$  V, IP and EA of 6.25 and 3.65 eV, respectively, are calculated for PFQ, its band gap energy (IP – EA) is determined as 2.60 eV.

The band gap energy calculated from IP and EA energy levels is a little bit smaller than that from the optical band gap. The optical absorption and the electrochemical measurements are physically different processes and the IP/EA values derived from the electrochemical measurements should be taken with caution, since they are often obtained under irreversible or quasi-reversible redox process conditions and may include kinetic factors, due to structural re-arrangements and mass transport.<sup>37</sup> For

these reasons, in this paper, the onset of the redox curve in the first cycle was used and all voltammetric measurements were performed using the oligomer in solution instead of its film deposited onto the electrode.

Table 1 shows the EA and IP, the LUMO and HOMO energy levels, respectively, and the band gap energy for PFQ, compared to other electroluminescent polymers from the literature. Apparently, this polymer can serve as an n-type conjugated polymer because of its low-lying LUMO level. On the other hand, the HOMO energy level of PFQ is very close to that observed for [6,6]-phenyl-C<sub>61</sub>-butyric acid methyl ester (PCBM) (6.10 eV),<sup>38</sup> only 0.15 eV lower, which points toward a potential application of PFQ as a donor material in bulk heterojunction solar cell devices with PCBM as acceptor. Additionally, the calculated electrochemical band gap indicates a blue luminescence for PFQ, as proved by fluorescence spectroscopy.

**Table 1.** Values of LUMO (EA), HOMO (IP) and band gap

Copolymer	EA/ eV	IP/ eV	Band gap / eV
PFQ	3.65	6.25	2.60
PBOQ <sup>39</sup>	2.82	5.96	3.14
P6BTQ <sup>40</sup>	2.94	5.44	2.50
MEH-PPV <sup>41</sup>	2.91	5.10	2.19

PFQ: poly[1,4-phenylene-2,7-(9,9-dioctyl-fluorenylene)-co-1,4-phenylene-5,7-(8-oxyoctyl-quinolinylene)]; PBOQ: Poly(2,2'-(4,4'-diphenylene)-6,6'-bis(4-octylquinoline)); P6BTQ: Poly(2,2'-(3,3'-dihexyl-2,2'-bithienylene-6,6'-bis(4-phenylquinoline)); MEH-PPV: poly[2-methoxy-5-(2'-ethylhexyloxy)-p-phenylene vinylene].

## Conclusions

A highly soluble novel material comprised of quinoline and fluorene units has been straightforwardly prepared using the Suzuki coupling reaction. The copolymer has been shown to present good photoluminescence behavior along with low LUMO energy level, suggesting its use as an n-type semiconductor, which means that PFQ can potentially function as an active layer in PLEDs without adding an ETL.

## Acknowledgments

The authors thank FAPESP (07/50742-2), CNPq, CAPES and INEO-INCT for financial support.

## References

- Burroughes, J. H.; Bradley, D. D. C.; Brown, A. R.; Marks, R. N.; Mackay, K.; Friend, R. H.; Burn, P. L.; Holmes, A. B.; *Nature* **1990**, *347*, 539.

2. Friend, R. H.; Gymer, R. W.; Holmes, A. B.; Burroughes, J. H.; Marks, R. N.; Taliani, C.; Bradley, D. D. C.; dos Santos, D. A.; Brédas, J. L.; Lögdlund, M.; Salaneck, W. R.; *Nature* **1999**, *397*, 121.
3. Blom, P. W. M.; Vissenberg, M. C. J. M.; *Mater. Sci. Eng., R* **2000**, *27*, 53.
4. Berntsen, A.; Croonen, Y.; Liedenbaum, C.; Schoo, H.; Visser, R.; Vleggaar, J.; Eijer, P.; *Opt. Mater.* **1998**, *9*, 125.
5. Blom, P. W. M.; Berntsen, A. J. M.; *J. Mater. Sci.* **2000**, *11*, 105.
6. Hung, L. S.; Chen, C. H.; *Mater. Sci. Eng., R* **2002**, *39*, 143.
7. Bangcuyo, C. G.; Rampey, V. M. E.; Quan, L. T.; Angel, S. M.; Smith, M. D.; Bunz, U. H. F.; *Macromolecules* **2002**, *35*, 1563.
8. Zhang, X.; Shetty, A. S.; Jenekhe, S. A.; *Macromolecules* **1999**, *32*, 7422.
9. Lu, L.; Jenekhe, S. A.; *Macromolecules* **2001**, *34*, 6249.
10. Alam, M. M.; Jenekhe, S. A.; *J. Phys. Chem. B* **2001**, *105*, 2479.
11. Zhu, Y.; Alam, M. M.; Jenekhe, S. A.; *Macromolecules* **2002**, *35*, 9844.
12. Simas, E. R.; Martins, T. D.; Atvars, T. D. Z.; Akcelrud, L.; *J. Lumin.* **2009**, *129*, 119.
13. Liu, Y.; Ma, H.; Jen, A. K.-Y.; *J. Mater. Chem.* **2001**, *11*, 1800.
14. Kim, D. Y.; *Synth. Met.* **2001**, *121*, 1707.
15. Neher, D.; *Macromol. Rapid Commun.* **2001**, *22*, 1365.
16. Leclerc, M.; *J. Polym. Sci., Part A: Polym. Chem.* **2001**, *39*, 2867.
17. Scherf, U.; List, E. J. W.; *Adv. Mater.* **2002**, *14*, 477.
18. Klaerner, G.; Miller, R. D.; *Macromolecules* **1998**, *31*, 2007.
19. Kim, D. Y.; Lee, S. K.; Kim, S. L.; Kim, J. K.; Lee, H.; Cho, H. N.; Hong, S. I.; Kim, C. Y.; *Synth. Met.* **2001**, *121*, 1707.
20. Su, H. J.; Wu, F. I.; Shu, C. F.; Tung, Y. L.; Chi, Y.; Lee, G. H.; *J. Polym. Sci., Part A: Polym. Chem.* **2005**, *43*, 859.
21. Chen, C. H.; Shu, C. F.; *J. Polym. Sci., Part A: Polym. Chem.* **2004**, *42*, 3314.
22. Miyaura, N.; Suzuki, A.; *Chem. Rev.* **1995**, *95*, 2457.
23. Suzuki, A.; *J. Organomet. Chem.* **1999**, *576*, 147.
24. Kotha, S.; Lahiri, K.; Kashinath, D.; *Tetrahedron* **2002**, *58*, 9633.
25. Wang, S. H.; Correia, F. C.; Br PI 1.002.492-1, 2010.
26. Correia, F. C.; Wang, S. H.; Péres, L. O.; Caseli, L.; *Colloids Surf., A* **2012**, *394*, 67.
27. Santos, T. C. F.; Péres, L. O.; Wang, S. H.; Oliveira Jr., O. N.; Caseli, L.; *Langmuir* **2010**, *98*, 5869.
28. Liu, B.; Yu, W.-L.; Lai, Y.-H.; Huang, W.; *Chem. Mater.* **2001**, *13*, 1984.
29. Fukuda, M.; Sawada, K.; Yoshino, K.; *J. Polym. Sci., Part A: Polym. Chem.* **1993**, *31*, 2465.
30. Zhan, X.; Liu, Y.; Wu, X.; Wang, S.; Zhu, D.; *Macromolecules* **2002**, *35*, 2529.
31. Bree, A.; Zwarich, R.; *J. Chem. Phys.* **1969**, *51*, 903.
32. Pavlopoulos, T. G.; *Spectrochim. Acta, Part A* **1986**, *42*, 1307.
33. Park, J. W.; Park, S. J.; Kim, Y. H.; Shin, D. C.; You, H.; Kwon, S. K.; *Polymer* **2009**, *50*, 102.
34. Garcia, J. R.; Peres, L. O.; Fernandes, M. R.; Gruber, J.; Nart, F. C.; *J. Solid State Electrochem.* **2004**, *8*, 122.
35. Andruzzi, R.; Trazza, A.; Greci, L.; Marchetti, L. J.; *Electroanal. Chem.* **1980**, *108*, 59.
36. Ponomarev, O. A.; Brusiltsev, Y. N.; Kotelevskii, S. I.; Mitina, V. G.; Pedash, Y. F.; *Theor. Exp. Chem.* **1990**, *26*, 605.
37. Miteva, T.; Meisel, A.; Knoll, W.; Nothofer, H. G.; Scherf, U.; Müller, D. C.; Meerholz, K.; Yasuda, A.; Neher, D.; *Adv. Mater.* **2001**, *13*, 565.
38. Chen, H. Y.; Hou, J.; Zhang, S.; Liang, Y.; Yang, G.; Yang, Y.; Yu, L.; Wu, Y.; Li, G.; *Nat. Photonics* **2009**, *3*, 649.
39. Tonzola, C. J.; Alam, M. M.; Jenekhe, S. A.; *Macromolecules* **2005**, *38*, 9539.
40. Tonzola, C. J.; Alam, M. M.; Bean, B. A.; Jenekhe, S. A.; *Macromolecules* **2004**, *37*, 3554.
41. Swager, T. M.; Izuhara, D.; *J. Am. Chem. Soc.* **2009**, *131*, 17724.

Submitted: May 27, 2014

Published online: September 19, 2014

FAPESP has sponsored the publication of this article.